Acta Cryst E CRYSTALLOGRAPHIC COMMUNICATIONS

ISSN 2056-9890

# (*E*)-1,3-Bis(anthracen-9-yl)prop-2-en-1-one: crystal structure and DFT study

**Dian Alwani Zainuri, Ibrahim Abdul Razak and Suhana Arshad***

X-ray Crystallography Unit, School of Physics, Universiti Sains Malaysia, 11800 USM, Penang, Malaysia. *Correspondence e-mail: suhanaarshad@usm.my

Received 12 February 2018
Accepted 5 March 2018

Edited by W. T. A. Harrison, University of Aberdeen, Scotland

**Keywords:** crystal structure; chalcone; absorption spectra; HOMO–LUMO; Hirshfeld surface.

**CCDC reference**: 1817217

**Supporting information**: this article has supporting information at journals.iucr.org/e

The title compound, $C_{31}H_{20}O$, was synthesized using a Claisen–Schmidt condensation. The enone group adopts an *s-trans* conformation and the anthracene ring systems are twisted at angles of 85.21 (19) and 83.98 (19)° from the enone plane. In the crystal, molecules are connected into chains along [100] *via* weak C—H···$\pi$ interactions. The observed band gap of 3.03 eV is in excellent agreement with that (3.07 eV) calculated using density functional theory (DFT) at the B3LYP/6–311++G(d,p) level. The Hirshfeld surface analysis indicates a high percentage of C···H/H···C (41.2%) contacts in the crystal.

## 1. Chemical context

Anthrancene and its derivatives constitute a very well-known class with interesting photophysical properties and they are used extensively in the design of luminescent chemosensors and switches (Montalti *et al.*, 2000). A chalcone molecule with a $\pi$-conjugated system provides a large charge-transfer axis with appropriate substituent groups on the terminal aromatic rings. Strong intermolecular charge transfer (ICT) will give rise to second harmonic generation (SHG) efficiency and this may enhance the non-linear optical (NLO) properties (D'silva *et al.*, 2011). Furthermore, $\pi$-conjugated molecular materials with fused rings are the focus of considerable interest in the emerging area of organic electronics, since the combination of good charge-carrier mobility and high stability may lead to potential optoelectronic applications (Wu *et al.*, 2010). As part of our work in this area, we now report the synthesis and combined experimental and theoretical studies of the title compound, (I).

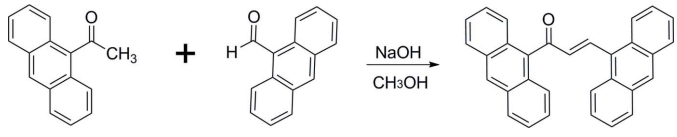


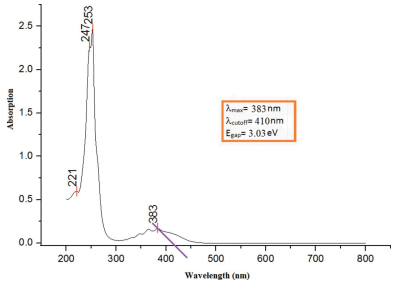


## 2. Structural commentary

The molecular structure of (I) is shown in Fig. 1 (for the optimized structure, see Fig. S1 in the Supporting information). The structure consists of two anthracene rings (Anth *A* and Anth *B*) . Anth *A* is formed by the aromatic rings labeled as *Cg*1(C1–C6), *Cg*2(C1/C6–C8/C13/C14) and *Cg*3(C8–C13). Anth *B* consists of *Cg*4(C18/C19/C24–C26/C31, *Cg*5(C19–C24) and *Cg*6(C26–C31).

**Table 1**
Hydrogen-bond geometry (Å, °).

*Cg*4 and *Cg*6 are the centroids of the C18/C19/C24–C26/C31 and C26–C31 rings, respectively.

| *D*—H···*A* | *D*—H | H···*A* | *D*···*A* | *D*—H···*A* |
|---|---|---|---|---|
| C5—H5*A*···*Cg*4$^{i}$ | 0.93 | 2.75 | 3.511 (2) | 140 |
| C7—H7*A*···*Cg*6$^{i}$ | 0.93 | 2.91 | 3.672 (2) | 140 |

Symmetry code: (i) $x-1, y, z$.

The C—C distances in the central ring of the anthracene units show little variation compared to the other rings (Anth *A*: C20—C21, C22—C23, C27—C28 and C29—C30; Anth *B*: C2—C3, C4—C5, C9—C10 and C11—C12), which are much shorter. These observations are consistent with an electronic structure for the anthracene units where a central ring displaying aromatic delocalization is flanked by two isolated diene units (Glidewell & Lloyd, 1984). Both theoretical and experimental structures exist in an *E* configuration with respect to the C16═C17 double bond [experimental = 1.291 (2) Å and DFT (see below) = 1.34 Å].

The enone moiety (O1/C15–C17) shows an *s-trans* configuration with the O1—C15—C16—C17 torsion angle being −179.19 (19) and 179.64° in the experimental and calculated structures, respectively. Additionally, the enone moiety [O1/C15–C17, maximum deviation of 0.0039 (18) Å at C16] forms dihedral angles of 85.21 (19) and 83.98 (19)° with the Anth *A* [C1–C14, maximum deviation of 0.103 (2) Å at C11] and Anth *B* [C18–C31, maximum deviation of 0.016 (3) Å at C27] groups, respectively. The large dihedral-angle deviation indicates that the possibility for electronic effects between the anthracene units through the enone moiety has decreased (Jung *et al.*, 2008). This is in contrast with the molecular structure of (*E*)-1-(anthracen-9-yl)-3-(2-chloro-6-fluorophenyl)prop-2-en-1-one (Abdullah *et al.* 2016), which shows the enone moiety locked in an *s-cis* configuration because of the intramolecular hydrogen bond. Furthermore, the bulkiness of the anthracene ring gives rise to a highly twisted structure at both terminal rings. Compound (I) is twisted at the C17—C18 and C14—C15 bonds with C16—C17—C18—C19 and C1—C14—C15—C16 torsion angles of 84.0 (2) and 93.65 (19)°, respectively (see Fig. S2 in the Supporting information). The corresponding torsion angles for the DFT study are 48.01 and 94.05°, respectively. We propose that the torsion-angle difference of about 35.9° between the experimental and DFT studies are the result of the formation of intermolecular C—H···$\pi$ interactions involving the anthracene units. The observed intermolecular interactions in the crystal packing are the main cause of the angle difference when this interaction is not taken into consideration during the optimization process.

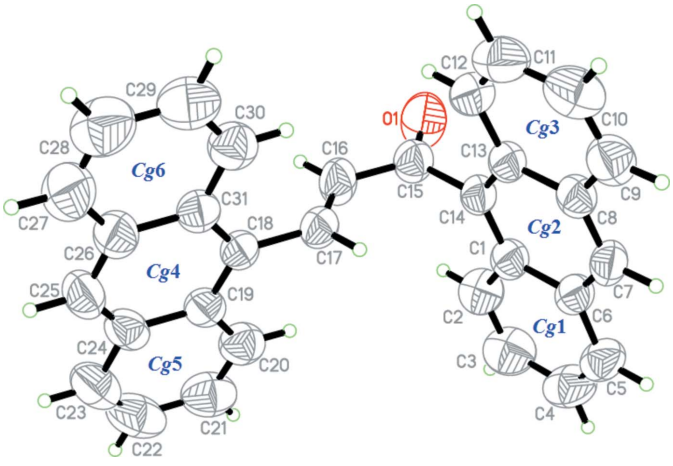


**Figure 1**
The molecular structure of (I) showing 50% displacement ellipsoids.

## 3. Supramolecular features

In the crystal of (I), C—H···$\pi$ interactions are mainly responsible for the packing. Two C—H···$\pi$ interactions (Fig. 2 and Table 1) occur between anthracene rings (Anth *A* and Anth *B*), connecting the molecules into infinite zigzag chains propagating along the [100] direction.

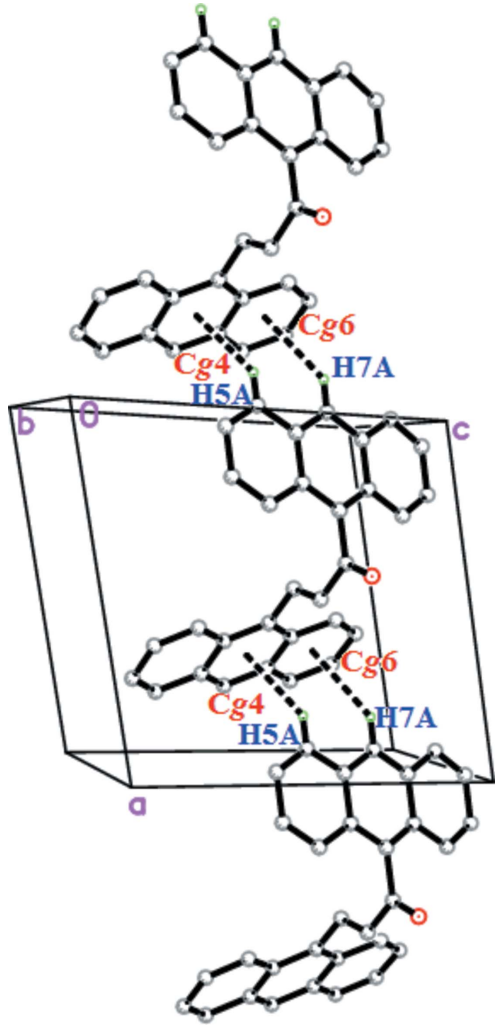


**Figure 2**
The weak C—H···$\pi$ interactions in the crystal of (I).

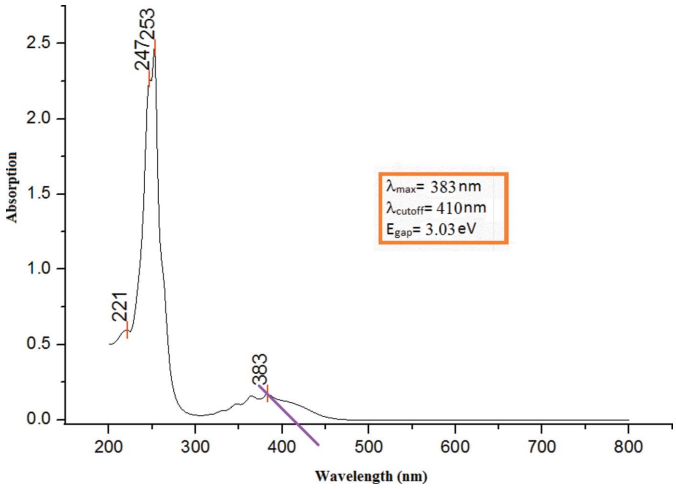


**Figure 3**
UV–Vis absorption spectra of (I).

## 4. Theoretical chemistry study

The optimization of the molecular geometries leading to energy minima was achieved using DFT [with Becke's non-local three parameter exchange and the Lee–Yang–Parr correlation functional (B3LYP)] with the 6-311++G (d,p) basis set as implemented in *Gaussian09* program package (Frisch *et al.*, 2009). The selected bond lengths and angles of the optimized structure in comparison to the experimental values are presented in Table S2 in the Supporting information and the optimized structure is presented in Figure S1. Agreement between experimental and calculated geometrical data is generally good and any deviations may be ascribed to the fact that the optimization is performed in an isolated condition, whereas the crystal environment affects the molecular geometry (Ramya *et al.*, 2015).

## 5. Absorption spectrum and frontier molecular orbitals

The longest wavelength absorption maxima for (I) is observed in the UV region at 383 nm as shown in Fig. 3. The TD–DFT calculation at the B3LYP/6-311G++(d,p) level shows that this feature is due to an electronic transition from the highest occupied molecular orbital (HOMO) to the lowest unoccupied molecular orbital (LUMO). In the ground state (HOMO), the charge densities are mainly delocalized over the anthracene rings and the enone moiety, while in the LUMO state, the charge densities are accumulated on the Anth *A* and enone moiety (see Fig. S3 in the Supporting information). The calculated $\lambda_{max}$ of 390 nm is shifted from the experimental value, which may be attributed to solvent effects, compared to the gas-phase calculation.

The HOMO–LUMO energy gap (Fig. S3) relates to the chemical activity of the molecule (Kosar & Albayrak, 2011). The predicted energy gap of 3.07 eV shows excellent agreement with the estimated experimental energy gap of 3.03 eV. These optical band-gap values indicate the potential suitability of this compound for optoelectronic applications, as previously reported by Prabhu *et al.* (2016). Additionally, Nietfeld *et al.* (2011) compared the structural, electrochemical and optical properties of fused-ring and non-fused ring compounds, indicating that fused rings have lower band gaps than other structures.

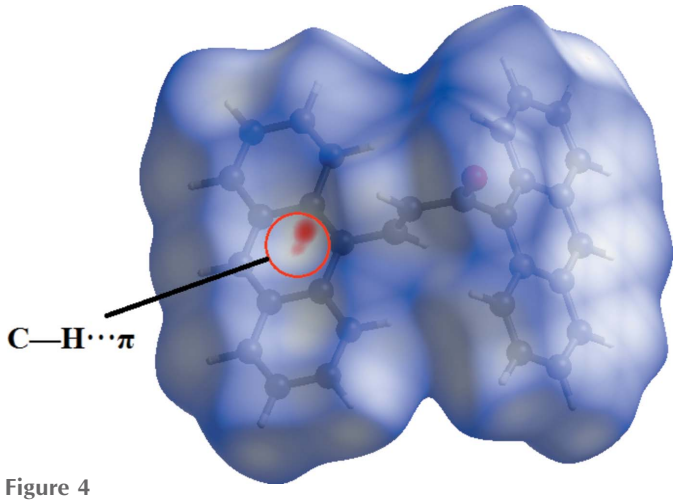


**Figure 4**
View of the Hirshfeld surfaces mapped over $d_{norm}$ for (I).

## 6. Hirshfeld Surface analysis

Fig. 4 shows the Hirshfeld surface mapped over $d_{norm}$. As expected, the $d_{norm}$ surfaces reveal the C—H···$\pi$ intermolecular interaction as a large depression (bright-red spot). The presence of this C—H···$\pi$ interaction is also indicated through the combination of pale-orange and bright-red spots that are present on the Hirshfeld surfaces mapped over $d_e$ (Fig. 5*a*) and shape-index (Fig. 5*b*).

The two-dimensional fingerprint plots shown in Fig. 6 illustrate the difference between the intermolecular interaction patterns and the major intermolecular contacts associated with the title compound. The H···H contacts (Fig. 6*b*) appear to be the major contributor to the Hirshfeld surface and are seen as one distinct spike with a minimum value for $d_e + d_i$ that is less than the sum of the van der Waals radii (2.4 Å). The intermolecular C—H···$\pi$ interactions are characterized by the short interatomic C···H/H···C (41.2%) contacts and

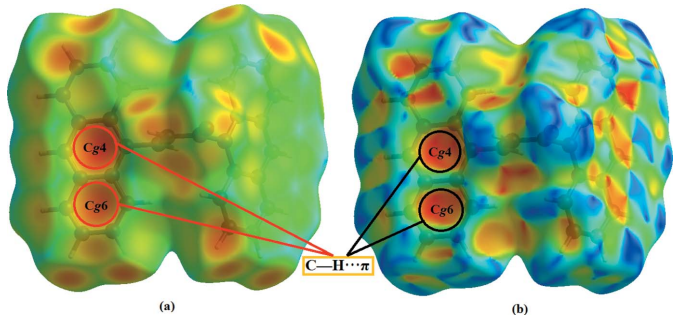


**Figure 5**
View of the Hirshfeld surfaces for (I) mapped over (*a*) $d_e$ and (*b*) shape-index with the pale-orange spot within the red circles showing the presence of the C—H···$\pi$ interactions.

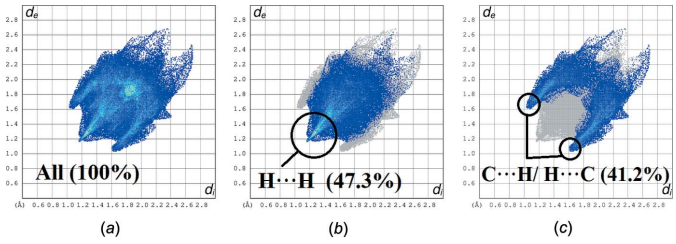


**Figure 6**
Fingerprint plots of interactions, listing the percentage of contacts (*a*) full two-dimensional fingerprint plots, and (*b*) H···H and (*c*) C···H/H···C contributions to the total Hirshfeld surface. The outline of the full fingerprint plots is shown in grey.

their presence is indicated by the distribution of points around a pair of wings at $d_e + d_i \sim 2.6$ Å (Fig. 6*c*).

## 7. Database survey

A survey of the Cambridge Structural Database (CSD, Version 5.38, last update Nov 2016; Groom *et al.*, 2016) revealed fused-ring substituted chalcones similar to the title compound. There are four compounds which have an anthracene-ketone subtituent on the chalcone: 9-anthryl styryl ketone and 9,10-anthryl bis(styryl ketone) (Harlow *et al.*, 1975), (2*E*)-1-(anthracen-9-yl)-3-[4-(propan-2-yl)phenyl]-prop-2-en-1-one (Girisha *et al.*, 2016) and (*E*)-1-(anthracen-9-yl)-3-(2-chloro-6-fluorophenyl) prop-2-en-1-one (Abdullah *et al.*, 2016). Jung *et al.* (2008) reported two ferrocenyl chalcones containing an anthracenyl subtituent, 9-(2-ferrocenylethenyl-carbonyl)anthracene and 1-(9-anthracenyl)-3-ferrocenyl-2-propen-1-one. Other related compounds include, 1-(anthracen-9-yl)-2-methylprop-2-en-1-one (Agrahari *et al.*, 2015) and 9-anthroylacetone (Cicogna *et al.*, 2004).

## 8. Synthesis and crystallization

A mixture of 9-acetylanthracene (0.5 mmol) and 9-anthracenecarboxaldehyde (0.5 mmol) was dissolved in methanol (20 ml). A catalytic amount of NaOH (5 ml, 20%) was added to the solution dropwise with vigorous stirring. The reaction mixture was stirred for about 5-6 h at room temperature. After stirring, the contents of the flask were poured into ice-cold water (50 ml). The resultant crude products were filtered, washed successively with distilled water and recrystallized from acetone solution as yellow blocks. The single crystal (Fig. S4) used for data collection was obtained by the slow-evaporation technique using acetone as the solvent.

## 9. Refinement

Crystal data collection and structure refinement details are summarized in Table 2. All H atoms were positioned geometrically (C—H =0.93 Å) and refined using riding model with $U_{iso}$(H)=1.2$U_{eq}$(C).

**Table 2**
Experimental details.

| | |
|---|---|
| Crystal data | |
| Chemical formula | $C_{31}H_{20}O$ |
| $M_r$ | 408.47 |
| Crystal system, space group | Triclinic, $P\overline{1}$ |
| Temperature (K) | 296 |
| *a*, *b*, *c* (Å) | 9.8310 (17), 10.7521 (18), 11.3029 (19) |
| $\alpha$, $\beta$, $\gamma$ (°) | 67.146 (2), 73.586 (2), 78.768 (2) |
| $V$ (Å$^3$) | 1051.2 (3) |
| $Z$ | 2 |
| Radiation type | Mo $K\alpha$ |
| $\mu$ (mm$^{-1}$) | 0.08 |
| Crystal size (mm) | 0.45 × 0.38 × 0.26 |
| | |
| Data collection | |
| Diffractometer | Bruker SMART APEXII DUO CCD area-detector |
| Absorption correction | Multi-scan (*SADABS*; Bruker, 2009) |
| No. of measured, independent and observed [$I > 2\sigma(I)$] reflections | 42832, 6216, 2792 |
| $R_{int}$ | 0.047 |
| (sin $\theta/\lambda)_{max}$ (Å$^{-1}$) | 0.709 |
| | |
| Refinement | |
| $R[F^2 > 2\sigma(F^2)]$, $wR(F^2)$, $S$ | 0.057, 0.187, 1.00 |
| No. of reflections | 6216 |
| No. of parameters | 289 |
| H-atom treatment | H-atom parameters constrained |
| $\Delta\rho_{max}$, $\Delta\rho_{min}$ (e Å$^{-3}$) | 0.20, −0.15 |

Computer programs: *APEX2* and *SAINT* (Bruker, 2009), *SHELXL2013* (Sheldrick, 2015), *SHELXTL* (Sheldrick, 2008) and *PLATON* (Spek, 2009).


## Funding information

The authors thank the Malaysian Government and Universiti Sains Malaysia (USM) for the research facilities and the Fundamental Research Grant Scheme (FRGS) No. 203/PFIZIK/6711572 and for Short Term Grant Scheme (304/PFIZIK/6313336) to conduct this work. DAZ thanks the Malaysian Government for the My Brain15 scholarship.


## References


Abdullah, A. A., Hassan, N. H. H., Arshad, S., Khalib, N. C. & Razak, I. A. (2016). *Acta Cryst.* E**72**, 648–651.
Agrahari, A., Wagers, P. O., Schildcrout, S. M., Masnovi, J. & Youngs, W. J. (2015). *Acta Cryst.* E**71**, 357–359.
Bruker (2009). *APEX2*, *SAINT* and *SADABS*. Bruker AXS Inc., Madison, Wisconsin, USA.
Cicogna, F., Ingrosso, G., Lodato, F., Marchetti, F. & Zandomeneghi, M. (2004). *Tetrahedron*, **60**, 11959–11968.
D'silva, E. D., Podagatlapalli, G. K., Rao, S. V., Rao, D. N. & Dharmaprakash, S. M. (2011). *Cryst. Growth Des.* **11**, 5362–5369.
Frisch, M. J., *et al.* (2009). *Gaussian 09*. Gaussian, Inc., Wallingford CT, USA.
Girisha, M., Yathirajan, H. S., Jasinski, J. P. & Glidewell, C. (2016). *Acta Cryst.* E**72**, 1153–1158.
Glidewell, C. & Lloyd, D. (1984). *Tetrahedron*, **40**, 4455–4472.
Groom, C. R., Bruno, I. J., Lightfoot, M. P. & Ward, S. C. (2016). *Acta Cryst*. B**72**, 171–179.
Harlow, R. L., Loghry, R. A., Williams, H. J. & Simonsen, S. H. (1975). *Acta Cryst.* B**31**, 1344–1350.

Jung, Y., Son, K., Oh, Y. E. & Noh, D. (2008). *Polyhedron*, **27**, 861–867.
Kosar, B. & Albayrak, C. (2011). *Spectrochim. Acta A Mol. Biomol. Spectrosc.* **78**, 160–167.
Montalti, M., Prodi, L. & Zaccheroni, N. (2000). *J. Fluoresence*, **10**, 71–76.
Nietfeld, J. P., Schwiderski, R. L., Gonnella, T. P. & Rasmussen, S. C. (2011). *J. Org. Chem.* **76**, 6383–6388.
Prabhu, A. N., Upadhyaya, V., Jayarama, A. & Bhat, K. B. (2016). *Mol. Cryst. Liq. Cryst.* **637**, 76–86.
Ramya, T., Gunasekaran, S. & Ramkumaar, G. R. (2015). *Spectrochim. Acta A Mol. Biomol. Spectrosc.* **149**, 132–142.
Sheldrick, G. M. (2008). *Acta Cryst*. A**64**, 112–122.
Sheldrick, G. M. (2015). *Acta Cryst*. C**71**, 3–8.
Spek, A. L. (2009). *Acta Cryst*. D**65**, 148–155.
Wu, W., Liu, Y. & Zhu, D. (2010). *Chem. Soc. Rev.* **39**, 1489–1502.

# supporting information

*Acta Cryst.* (2018). E**74**, 492-496 [https://doi.org/10.1107/S2056989018003791]

## (*E*)-1,3-Bis(anthracen-9-yl)prop-2-en-1-one: crystal structure and DFT study

**Dian Alwani Zainuri, Ibrahim Abdul Razak and Suhana Arshad**

### Computing details

Data collection: *APEX2* (Bruker, 2009); cell refinement: *SAINT* (Bruker, 2009); data reduction: *SAINT* (Bruker, 2009); program(s) used to solve structure: *SHELXTL* (Sheldrick, 2008); program(s) used to refine structure: *SHELXL2013* (Sheldrick, 2015); molecular graphics: *SHELXTL* (Sheldrick, 2008); software used to prepare material for publication: *SHELXTL* (Sheldrick, 2008) and *PLATON* (Spek, 2009).

### (*E*)-1,3-Bis(anthracen-9-yl)prop-2-en-1-one

*Crystal data*

$C_{31}H_{20}O$
$M_r$ = 408.47
Triclinic, $P\overline{1}$
$a$ = 9.8310 (17) Å
$b$ = 10.7521 (18) Å
$c$ = 11.3029 (19) Å
$\alpha$ = 67.146 (2)°
$\beta$ = 73.586 (2)°
$\gamma$ = 78.768 (2)°
$V$ = 1051.2 (3) Å$^3$
$Z$ = 2
$F(000)$ = 428
$D_x$ = 1.290 Mg m$^{-3}$
Mo $K\alpha$ radiation, $\lambda$ = 0.71073 Å
Cell parameters from 3766 reflections
$\theta$ = 2.3–22.1°
$\mu$ = 0.08 mm$^{-1}$
$T$ = 296 K
Block, yellow
0.45 × 0.38 × 0.26 mm

*Data collection*

Bruker SMART APEXII DUO CCD area-detector diffractometer
Radiation source: fine-focus sealed tube
$\varphi$ and $\omega$ scans
Absorption correction: multi-scan (*SADABS*; Bruker, 2009)
42832 measured reflections
6216 independent reflections
2792 reflections with $I > 2\sigma(I)$
$R_{int}$ = 0.047
$\theta_{max}$ = 30.3°, $\theta_{min}$ = 2.0°
$h$ = −13→13
$k$ = −15→15
$l$ = −15→15

*Refinement*

Refinement on $F^2$
Least-squares matrix: full
$R[F^2 > 2\sigma(F^2)]$ = 0.057
$wR(F^2)$ = 0.187
$S$ = 1.00
6216 reflections
289 parameters
0 restraints
Hydrogen site location: inferred from neighbouring sites
H-atom parameters constrained
$w = 1/[\sigma^2(F_o^2) + (0.0746P)^2 + 0.1037P]$ where $P = (F_o^2 + 2F_c^2)/3$
$(\Delta/\sigma)_{max} < 0.001$
$\Delta\rho_{max}$ = 0.20 e Å$^{-3}$
$\Delta\rho_{min}$ = −0.15 e Å$^{-3}$

*Special details*

**Geometry**. All esds (except the esd in the dihedral angle between two l.s. planes) are estimated using the full covariance matrix. The cell esds are taken into account individually in the estimation of esds in distances, angles and torsion angles; correlations between esds in cell parameters are only used when they are defined by crystal symmetry. An approximate (isotropic) treatment of cell esds is used for estimating esds involving l.s. planes.

*Fractional atomic coordinates and isotropic or equivalent isotropic displacement parameters (Å²)*

| | *x* | *y* | *z* | $U_{iso}$*/$U_{eq}$ |
|---|---|---|---|---|
| O1 | 0.44003 (14) | 0.39564 (13) | 0.83904 (17) | 0.0974 (5) |
| C1 | 0.18125 (17) | 0.58896 (16) | 0.72383 (17) | 0.0557 (4) |
| C2 | 0.2456 (2) | 0.55577 (19) | 0.6096 (2) | 0.0745 (5) |
| H2A | 0.3398 | 0.5184 | 0.5977 | 0.089* |
| C3 | 0.1725 (3) | 0.5774 (2) | 0.5176 (2) | 0.0895 (6) |
| H3A | 0.2174 | 0.5560 | 0.4428 | 0.107* |
| C4 | 0.0287 (3) | 0.6321 (2) | 0.5335 (2) | 0.0848 (6) |
| H4A | −0.0202 | 0.6472 | 0.4690 | 0.102* |
| C5 | −0.0372 (2) | 0.66204 (17) | 0.6411 (2) | 0.0702 (5) |
| H5A | −0.1325 | 0.6962 | 0.6513 | 0.084* |
| C6 | 0.03472 (17) | 0.64307 (16) | 0.74020 (18) | 0.0564 (4) |
| C7 | −0.03088 (16) | 0.67773 (16) | 0.84986 (18) | 0.0589 (4) |
| H7A | −0.1270 | 0.7093 | 0.8621 | 0.071* |
| C8 | 0.04251 (16) | 0.66686 (15) | 0.94246 (17) | 0.0551 (4) |
| C9 | −0.0227 (2) | 0.70868 (18) | 1.05166 (19) | 0.0707 (5) |
| H9A | −0.1189 | 0.7397 | 1.0651 | 0.085* |
| C10 | 0.0525 (3) | 0.7042 (2) | 1.1362 (2) | 0.0834 (6) |
| H10A | 0.0083 | 0.7335 | 1.2065 | 0.100* |
| C11 | 0.1973 (2) | 0.6556 (2) | 1.1191 (2) | 0.0776 (5) |
| H11A | 0.2487 | 0.6544 | 1.1772 | 0.093* |
| C12 | 0.26246 (19) | 0.61070 (18) | 1.01937 (18) | 0.0659 (5) |
| H12A | 0.3577 | 0.5762 | 1.0115 | 0.079* |
| C13 | 0.18947 (16) | 0.61474 (15) | 0.92571 (16) | 0.0529 (4) |
| C14 | 0.25475 (16) | 0.57424 (15) | 0.81840 (16) | 0.0528 (4) |
| C15 | 0.40796 (17) | 0.51694 (18) | 0.80046 (18) | 0.0633 (5) |
| C16 | 0.51726 (17) | 0.61184 (17) | 0.73382 (18) | 0.0666 (5) |
| H16A | 0.6119 | 0.5756 | 0.7213 | 0.080* |
| C17 | 0.49221 (16) | 0.74227 (16) | 0.69108 (16) | 0.0564 (4) |
| H17A | 0.3972 | 0.7775 | 0.7032 | 0.068* |
| C18 | 0.59990 (15) | 0.84051 (15) | 0.62495 (16) | 0.0510 (4) |
| C19 | 0.65765 (16) | 0.87661 (16) | 0.48951 (17) | 0.0547 (4) |
| C20 | 0.6174 (2) | 0.82323 (19) | 0.40902 (19) | 0.0701 (5) |
| H20A | 0.5499 | 0.7606 | 0.4473 | 0.084* |
| C21 | 0.6744 (2) | 0.8611 (2) | 0.2788 (2) | 0.0881 (6) |
| H21A | 0.6459 | 0.8247 | 0.2282 | 0.106* |
| C22 | 0.7768 (3) | 0.9552 (2) | 0.2183 (2) | 0.0955 (7) |
| H22A | 0.8155 | 0.9807 | 0.1280 | 0.115* |
| C23 | 0.8190 (2) | 1.0082 (2) | 0.2896 (2) | 0.0830 (6) |
| H23A | 0.8875 | 1.0697 | 0.2480 | 0.100* |

| | | | | |
|---|---|---|---|---|
| C24 | 0.76171 (18) | 0.97267 (17) | 0.42761 (18) | 0.0634 (5) |
| C25 | 0.80165 (19) | 1.02850 (18) | 0.5019 (2) | 0.0720 (5) |
| H25A | 0.8687 | 1.0914 | 0.4605 | 0.086* |
| C26 | 0.74538 (19) | 0.99421 (17) | 0.6362 (2) | 0.0658 (5) |
| C27 | 0.7864 (3) | 1.0506 (2) | 0.7140 (3) | 0.0899 (7) |
| H27A | 0.8524 | 1.1146 | 0.6740 | 0.108* |
| C28 | 0.7316 (3) | 1.0133 (2) | 0.8443 (3) | 0.0980 (7) |
| H28A | 0.7605 | 1.0513 | 0.8933 | 0.118* |
| C29 | 0.6313 (2) | 0.9178 (2) | 0.9075 (2) | 0.0841 (6) |
| H29A | 0.5946 | 0.8925 | 0.9981 | 0.101* |
| C30 | 0.58805 (19) | 0.86234 (18) | 0.83782 (19) | 0.0676 (5) |
| H30A | 0.5211 | 0.7994 | 0.8812 | 0.081* |
| C31 | 0.64201 (16) | 0.89751 (15) | 0.70003 (17) | 0.0555 (4) |

*Atomic displacement parameters (Å²)*

| | $U^{11}$ | $U^{22}$ | $U^{33}$ | $U^{12}$ | $U^{13}$ | $U^{23}$ |
|---|---|---|---|---|---|---|
| O1 | 0.0731 (9) | 0.0536 (8) | 0.1465 (14) | −0.0020 (6) | −0.0287 (9) | −0.0149 (8) |
| C1 | 0.0544 (9) | 0.0476 (9) | 0.0641 (11) | −0.0107 (7) | −0.0152 (8) | −0.0149 (8) |
| C2 | 0.0757 (12) | 0.0749 (13) | 0.0775 (13) | −0.0077 (10) | −0.0177 (10) | −0.0317 (11) |
| C3 | 0.1108 (18) | 0.0908 (16) | 0.0807 (15) | −0.0134 (13) | −0.0278 (13) | −0.0390 (12) |
| C4 | 0.1070 (17) | 0.0767 (14) | 0.0872 (16) | −0.0140 (12) | −0.0502 (14) | −0.0245 (12) |
| C5 | 0.0702 (11) | 0.0582 (11) | 0.0882 (14) | −0.0115 (8) | −0.0370 (11) | −0.0167 (10) |
| C6 | 0.0543 (9) | 0.0445 (9) | 0.0702 (11) | −0.0120 (7) | −0.0225 (8) | −0.0109 (8) |
| C7 | 0.0435 (8) | 0.0515 (9) | 0.0758 (12) | −0.0082 (7) | −0.0146 (8) | −0.0140 (8) |
| C8 | 0.0526 (9) | 0.0454 (9) | 0.0602 (10) | −0.0105 (7) | −0.0106 (8) | −0.0099 (7) |
| C9 | 0.0670 (11) | 0.0653 (12) | 0.0684 (12) | −0.0033 (9) | −0.0078 (10) | −0.0186 (9) |
| C10 | 0.1013 (16) | 0.0763 (14) | 0.0656 (13) | −0.0026 (12) | −0.0139 (12) | −0.0242 (10) |
| C11 | 0.0948 (15) | 0.0772 (13) | 0.0635 (12) | −0.0098 (11) | −0.0296 (11) | −0.0190 (10) |
| C12 | 0.0628 (10) | 0.0655 (11) | 0.0650 (12) | −0.0092 (8) | −0.0222 (9) | −0.0118 (9) |
| C13 | 0.0485 (8) | 0.0464 (9) | 0.0583 (10) | −0.0116 (7) | −0.0135 (7) | −0.0086 (7) |
| C14 | 0.0454 (8) | 0.0484 (9) | 0.0593 (10) | −0.0095 (6) | −0.0121 (7) | −0.0111 (8) |
| C15 | 0.0544 (9) | 0.0546 (10) | 0.0756 (12) | −0.0044 (8) | −0.0167 (8) | −0.0166 (9) |
| C16 | 0.0412 (8) | 0.0584 (11) | 0.0867 (13) | 0.0004 (7) | −0.0092 (8) | −0.0175 (9) |
| C17 | 0.0419 (8) | 0.0567 (10) | 0.0652 (11) | −0.0010 (7) | −0.0133 (7) | −0.0171 (8) |
| C18 | 0.0399 (7) | 0.0478 (9) | 0.0582 (10) | 0.0023 (6) | −0.0125 (7) | −0.0134 (7) |
| C19 | 0.0481 (8) | 0.0498 (9) | 0.0575 (10) | 0.0041 (7) | −0.0113 (7) | −0.0144 (8) |
| C20 | 0.0672 (11) | 0.0724 (12) | 0.0659 (12) | 0.0017 (9) | −0.0162 (9) | −0.0228 (10) |
| C21 | 0.0967 (16) | 0.0941 (16) | 0.0701 (14) | 0.0103 (13) | −0.0219 (12) | −0.0325 (12) |
| C22 | 0.1056 (18) | 0.0903 (16) | 0.0582 (13) | 0.0117 (13) | −0.0007 (12) | −0.0146 (12) |
| C23 | 0.0759 (13) | 0.0669 (13) | 0.0733 (14) | −0.0007 (10) | 0.0034 (11) | −0.0072 (11) |
| C24 | 0.0568 (10) | 0.0500 (10) | 0.0634 (11) | 0.0030 (8) | −0.0074 (8) | −0.0071 (8) |
| C25 | 0.0629 (11) | 0.0528 (10) | 0.0829 (14) | −0.0129 (8) | −0.0105 (10) | −0.0064 (10) |
| C26 | 0.0638 (10) | 0.0507 (10) | 0.0796 (13) | −0.0066 (8) | −0.0209 (10) | −0.0160 (9) |
| C27 | 0.1027 (16) | 0.0627 (13) | 0.1131 (19) | −0.0197 (11) | −0.0405 (15) | −0.0240 (13) |
| C28 | 0.126 (2) | 0.0814 (15) | 0.109 (2) | −0.0107 (14) | −0.0510 (17) | −0.0402 (14) |
| C29 | 0.0993 (16) | 0.0847 (15) | 0.0747 (14) | 0.0017 (12) | −0.0278 (12) | −0.0343 (12) |
| C30 | 0.0658 (11) | 0.0691 (12) | 0.0658 (12) | −0.0019 (9) | −0.0154 (9) | −0.0235 (9) |

| | | | | | | |
|---|---|---|---|---|---|---|
| C31 | 0.0509 (9) | 0.0493 (9) | 0.0624 (11) | 0.0010 (7) | −0.0161 (8) | −0.0162 (8) |

*Geometric parameters (Å, º)*

| | | | |
|---|---|---|---|
| O1—C15 | 1.2109 (19) | C16—H16A | 0.9300 |
| C1—C14 | 1.397 (2) | C17—C18 | 1.473 (2) |
| C1—C2 | 1.416 (3) | C17—H17A | 0.9300 |
| C1—C6 | 1.433 (2) | C18—C19 | 1.396 (2) |
| C2—C3 | 1.349 (3) | C18—C31 | 1.403 (2) |
| C2—H2A | 0.9300 | C19—C20 | 1.418 (3) |
| C3—C4 | 1.411 (3) | C19—C24 | 1.431 (2) |
| C3—H3A | 0.9300 | C20—C21 | 1.343 (3) |
| C4—C5 | 1.333 (3) | C20—H20A | 0.9300 |
| C4—H4A | 0.9300 | C21—C22 | 1.406 (3) |
| C5—C6 | 1.418 (2) | C21—H21A | 0.9300 |
| C5—H5A | 0.9300 | C22—C23 | 1.335 (3) |
| C6—C7 | 1.380 (2) | C22—H22A | 0.9300 |
| C7—C8 | 1.389 (2) | C23—C24 | 1.422 (3) |
| C7—H7A | 0.9300 | C23—H23A | 0.9300 |
| C8—C9 | 1.417 (2) | C24—C25 | 1.374 (3) |
| C8—C13 | 1.432 (2) | C25—C26 | 1.385 (3) |
| C9—C10 | 1.346 (3) | C25—H25A | 0.9300 |
| C9—H9A | 0.9300 | C26—C27 | 1.419 (3) |
| C10—C11 | 1.404 (3) | C26—C31 | 1.431 (2) |
| C10—H10A | 0.9300 | C27—C28 | 1.340 (3) |
| C11—C12 | 1.344 (3) | C27—H27A | 0.9300 |
| C11—H11A | 0.9300 | C28—C29 | 1.401 (3) |
| C12—C13 | 1.421 (2) | C28—H28A | 0.9300 |
| C12—H12A | 0.9300 | C29—C30 | 1.345 (3) |
| C13—C14 | 1.391 (2) | C29—H29A | 0.9300 |
| C14—C15 | 1.501 (2) | C30—C31 | 1.416 (2) |
| C15—C16 | 1.461 (2) | C30—H30A | 0.9300 |
| C16—C17 | 1.291 (2) | | |
| | | | |
| C14—C1—C2 | 123.06 (16) | C15—C16—H16A | 117.6 |
| C14—C1—C6 | 119.19 (16) | C16—C17—C18 | 126.16 (14) |
| C2—C1—C6 | 117.74 (16) | C16—C17—H17A | 116.9 |
| C3—C2—C1 | 121.13 (19) | C18—C17—H17A | 116.9 |
| C3—C2—H2A | 119.4 | C19—C18—C31 | 120.92 (15) |
| C1—C2—H2A | 119.4 | C19—C18—C17 | 120.16 (15) |
| C2—C3—C4 | 120.9 (2) | C31—C18—C17 | 118.92 (15) |
| C2—C3—H3A | 119.6 | C18—C19—C20 | 123.09 (16) |
| C4—C3—H3A | 119.6 | C18—C19—C24 | 119.04 (16) |
| C5—C4—C3 | 120.04 (19) | C20—C19—C24 | 117.87 (16) |
| C5—C4—H4A | 120.0 | C21—C20—C19 | 121.5 (2) |
| C3—C4—H4A | 120.0 | C21—C20—H20A | 119.3 |
| C4—C5—C6 | 121.60 (19) | C19—C20—H20A | 119.3 |
| C4—C5—H5A | 119.2 | C20—C21—C22 | 120.5 (2) |

| | | | |
|---|---|---|---|
| C6—C5—H5A | 119.2 | C20—C21—H21A | 119.7 |
| C7—C6—C5 | 122.16 (16) | C22—C21—H21A | 119.7 |
| C7—C6—C1 | 119.23 (15) | C23—C22—C21 | 120.5 (2) |
| C5—C6—C1 | 118.59 (18) | C23—C22—H22A | 119.8 |
| C6—C7—C8 | 121.90 (15) | C21—C22—H22A | 119.8 |
| C6—C7—H7A | 119.0 | C22—C23—C24 | 121.5 (2) |
| C8—C7—H7A | 119.0 | C22—C23—H23A | 119.2 |
| C7—C8—C9 | 122.02 (16) | C24—C23—H23A | 119.2 |
| C7—C8—C13 | 119.12 (16) | C25—C24—C23 | 122.26 (19) |
| C9—C8—C13 | 118.85 (16) | C25—C24—C19 | 119.60 (17) |
| C10—C9—C8 | 121.02 (18) | C23—C24—C19 | 118.14 (19) |
| C10—C9—H9A | 119.5 | C24—C25—C26 | 122.21 (17) |
| C8—C9—H9A | 119.5 | C24—C25—H25A | 118.9 |
| C9—C10—C11 | 120.5 (2) | C26—C25—H25A | 118.9 |
| C9—C10—H10A | 119.8 | C25—C26—C27 | 122.71 (19) |
| C11—C10—H10A | 119.8 | C25—C26—C31 | 118.98 (17) |
| C12—C11—C10 | 120.56 (19) | C27—C26—C31 | 118.31 (19) |
| C12—C11—H11A | 119.7 | C28—C27—C26 | 121.1 (2) |
| C10—C11—H11A | 119.7 | C28—C27—H27A | 119.4 |
| C11—C12—C13 | 121.64 (18) | C26—C27—H27A | 119.4 |
| C11—C12—H12A | 119.2 | C27—C28—C29 | 120.8 (2) |
| C13—C12—H12A | 119.2 | C27—C28—H28A | 119.6 |
| C14—C13—C12 | 123.25 (15) | C29—C28—H28A | 119.6 |
| C14—C13—C8 | 119.31 (15) | C30—C29—C28 | 120.3 (2) |
| C12—C13—C8 | 117.42 (16) | C30—C29—H29A | 119.9 |
| C13—C14—C1 | 121.16 (15) | C28—C29—H29A | 119.9 |
| C13—C14—C15 | 120.13 (15) | C29—C30—C31 | 121.57 (19) |
| C1—C14—C15 | 118.69 (15) | C29—C30—H30A | 119.2 |
| O1—C15—C16 | 120.98 (16) | C31—C30—H30A | 119.2 |
| O1—C15—C14 | 120.98 (15) | C18—C31—C30 | 122.86 (15) |
| C16—C15—C14 | 118.03 (14) | C18—C31—C26 | 119.26 (16) |
| C17—C16—C15 | 124.87 (15) | C30—C31—C26 | 117.88 (16) |
| C17—C16—H16A | 117.6 | | |

| | | | |
|---|---|---|---|
| C14—C1—C2—C3 | −176.92 (17) | C14—C15—C16—C17 | 1.4 (3) |
| C6—C1—C2—C3 | 1.6 (3) | C15—C16—C17—C18 | 179.28 (17) |
| C1—C2—C3—C4 | −0.9 (3) | C16—C17—C18—C19 | 84.0 (2) |
| C2—C3—C4—C5 | −0.6 (3) | C16—C17—C18—C31 | −96.6 (2) |
| C3—C4—C5—C6 | 1.4 (3) | C31—C18—C19—C20 | −179.19 (14) |
| C4—C5—C6—C7 | 177.88 (16) | C17—C18—C19—C20 | 0.3 (2) |
| C4—C5—C6—C1 | −0.7 (3) | C31—C18—C19—C24 | 0.3 (2) |
| C14—C1—C6—C7 | −0.8 (2) | C17—C18—C19—C24 | 179.77 (14) |
| C2—C1—C6—C7 | −179.38 (14) | C18—C19—C20—C21 | 179.48 (16) |
| C14—C1—C6—C5 | 177.76 (14) | C24—C19—C20—C21 | 0.0 (3) |
| C2—C1—C6—C5 | −0.8 (2) | C19—C20—C21—C22 | 0.2 (3) |
| C5—C6—C7—C8 | −175.90 (14) | C20—C21—C22—C23 | 0.1 (3) |
| C1—C6—C7—C8 | 2.6 (2) | C21—C22—C23—C24 | −0.5 (3) |
| C6—C7—C8—C9 | 176.81 (14) | C22—C23—C24—C25 | −178.53 (18) |

| | | | |
|---|---|---|---|
| C6—C7—C8—C13 | −1.7 (2) | C22—C23—C24—C19 | 0.7 (3) |
| C7—C8—C9—C10 | −176.32 (16) | C18—C19—C24—C25 | −0.7 (2) |
| C13—C8—C9—C10 | 2.2 (3) | C20—C19—C24—C25 | 178.85 (15) |
| C8—C9—C10—C11 | −1.1 (3) | C18—C19—C24—C23 | −179.92 (15) |
| C9—C10—C11—C12 | −1.1 (3) | C20—C19—C24—C23 | −0.4 (2) |
| C10—C11—C12—C13 | 2.1 (3) | C23—C24—C25—C26 | 179.77 (16) |
| C11—C12—C13—C14 | 177.40 (16) | C19—C24—C25—C26 | 0.6 (3) |
| C11—C12—C13—C8 | −0.9 (2) | C24—C25—C26—C27 | 179.65 (17) |
| C7—C8—C13—C14 | −1.0 (2) | C24—C25—C26—C31 | −0.1 (3) |
| C9—C8—C13—C14 | −179.59 (14) | C25—C26—C27—C28 | −178.81 (19) |
| C7—C8—C13—C12 | 177.34 (14) | C31—C26—C27—C28 | 0.9 (3) |
| C9—C8—C13—C12 | −1.2 (2) | C26—C27—C28—C29 | −0.3 (4) |
| C12—C13—C14—C1 | −175.44 (14) | C27—C28—C29—C30 | −0.3 (3) |
| C8—C13—C14—C1 | 2.8 (2) | C28—C29—C30—C31 | 0.4 (3) |
| C12—C13—C14—C15 | 2.9 (2) | C19—C18—C31—C30 | −178.97 (14) |
| C8—C13—C14—C15 | −178.87 (14) | C17—C18—C31—C30 | 1.6 (2) |
| C2—C1—C14—C13 | 176.59 (14) | C19—C18—C31—C26 | 0.2 (2) |
| C6—C1—C14—C13 | −1.9 (2) | C17—C18—C31—C26 | −179.29 (14) |
| C2—C1—C14—C15 | −1.8 (2) | C29—C30—C31—C18 | 179.39 (16) |
| C6—C1—C14—C15 | 179.75 (14) | C29—C30—C31—C26 | 0.2 (3) |
| C13—C14—C15—O1 | 95.9 (2) | C25—C26—C31—C18 | −0.3 (2) |
| C1—C14—C15—O1 | −85.7 (2) | C27—C26—C31—C18 | 179.96 (15) |
| C13—C14—C15—C16 | −84.7 (2) | C25—C26—C31—C30 | 178.88 (15) |
| C1—C14—C15—C16 | 93.65 (19) | C27—C26—C31—C30 | −0.9 (2) |
| O1—C15—C16—C17 | −179.19 (19) | | |

*Hydrogen-bond geometry (Å, º)*

Cg4 and Cg6 are the centroids of the C18/C19/C24–C26/C31 and C26–C31 rings, respectively.

| *D*—H···*A* | *D*—H | H···*A* | *D*···*A* | *D*—H···*A* |
|---|---|---|---|---|
| C5—H5*A*···*Cg*4$^{i}$ | 0.93 | 2.75 | 3.511 (2) | 140 |
| C7—H7*A*···*Cg*6$^{i}$ | 0.93 | 2.91 | 3.672 (2) | 140 |

Symmetry code: (i) *x*−1, *y*, *z*.

*Comparison of experimental and calculated molecular geometry parameters (Å, °)*

| Parameters | Exp | DFT |
|---|---|---|
| C15—O1 | 1.21 (19) | 1.22 |
| C1—C14 | 1.40 (2) | 1.40 |
| C1—C2 | 1.42 (3) | 1.42 |
| C2—C3 | 1.35 (3) | 1.35 |
| C3—C4 | 1.41 (3) | 1.41 |
| C4—C5 | 1.33 (3) | 1.33 |
| C5—C6 | 1.42 (2) | 1.42 |
| C6—C7 | 1.380 (2) | 1.38 |
| C7—C8 | 1.39 (2) | 1.39 |
| C8—C9 | 1.42 (2) | 1.42 |
| C9—C10 | 1.35 (3) | 1.35 |

| | | |
|---|---|---|
| C10—C11 | 1.40 (3) | 1.40 |
| C11—C12 | 1.34 (3) | 1.34 |
| C12—C13 | 1.42 (2) | 1.42 |
| C13—C14 | 1.39 (2) | 1.39 |
| C14—C15 | 1.50 (2) | 1.52 |
| C15—C16 | 1.46 (2) | 1.48 |
| C16—C17 | 1.29 (2) | 1.35 |
| C17—C18 | 1.47 (2) | 1.47 |
| C18—C19 | 1.40 (2) | 1.40 |
| C19—C20 | 1.42 (3) | 1.42 |
| C20—C21 | 1.34 (3) | 1.34 |
| C21—C22 | 1.41 (3) | 1.41 |
| C22—C23 | 1.34 (3) | 1.34 |
| C23—C24 | 1.42 (3) | 1.42 |
| C24—C25 | 1.37 (3) | 1.37 |
| C25—C26 | 1.39 (3) | 1.38 |
| C26—C27 | 1.42 (3) | 1.42 |
| C27—C28 | 1.34 (3) | 1.34 |
| C28—C29 | 1.40 (3) | 1.40 |
| C29—C30 | 1.35 (3) | 1.35 |
| C30—C31 | 1.42 (2) | 1.42 |
| C31—C18 | 1.40 (2) | 1.40 |
| C14—C15—C16 | 118.03 (14) | 119.35 |
| O1—C15—C14 | 120.98 (15) | 120.25 |
| O1—C15—C16 | 120.98 (16) | 120.40 |
| C15—C16—C17 | 124.87 (15) | 123.93 |
| C16—C17—C18 | 126.16 (14) | 127.15 |